Geobiology (2009), 7, 155–170 DOI: 10.1111/j.1472-4669.2009.00195.x

The Eocene Arctic *Azolla* bloom: environmental conditions, productivity and carbon drawdown

E. N. SPEELMAN,[1] M. M. L. VAN KEMPEN,[2] J. BARKE,[3] H. BRINKHUIS,[3] G. J. REICHART,[1] A. J. P. SMOLDERS,[2] J. G. M. ROELOFS,[2] F. SANGIORGI,[3] J. W. DE LEEUW,[1,3,4] A. F. LOTTER[3] AND J. S. SINNINGHE DAMSTÉ[1,4]

[1]*Faculty of Geosciences, Utrecht University, Budapestlaan 4, 3584 CD Utrecht, The Netherlands*
[2]*Department of Aquatic Ecology and Environmental Biology, Faculty of Science, Radboud University, Heyendaalseweg 135, 6525 AJ, Nijmegen, The Netherlands*
[3]*Institute of Environmental Biology, Laboratory of Palaeobotany and Palynology, Utrecht University, Budapestlaan 4, 3584 CD Utrecht, The Netherlands*
[4]*NIOZ Royal Netherlands Institute for Sea Research, Department of Marine Organic Biogeochemistry, PO Box 59, 1790 AB Den Burg, Texel, The Netherlands*

ABSTRACT

Enormous quantities of the free-floating freshwater fern *Azolla* grew and reproduced *in situ* in the Arctic Ocean during the middle Eocene, as was demonstrated by microscopic analysis of microlaminated sediments recovered from the Lomonosov Ridge during Integrated Ocean Drilling Program (IODP) Expedition 302. The timing of the *Azolla* phase (~48.5 Ma) coincides with the earliest signs of onset of the transition from a greenhouse towards the modern icehouse Earth. The sustained growth of *Azolla*, currently ranking among the fastest growing plants on Earth, in a major anoxic oceanic basin may have contributed to decreasing atmospheric pCO_2 levels via burial of *Azolla*-derived organic matter. The consequences of these enormous *Azolla* blooms for regional and global nutrient and carbon cycles are still largely unknown. Cultivation experiments have been set up to investigate the influence of elevated pCO_2 on *Azolla* growth, showing a marked increase in *Azolla* productivity under elevated (760 and 1910 ppm) pCO_2 conditions. The combined results of organic carbon, sulphur, nitrogen content and ^{15}N and ^{13}C measurements of sediments from the *Azolla* interval illustrate the potential contribution of nitrogen fixation in a euxinic stratified Eocene Arctic. Flux calculations were used to quantitatively reconstruct the potential storage of carbon (0.9–3.5 10^{18} gC) in the Arctic during the *Azolla* interval. It is estimated that storing 0.9 10^{18} to 3.5 10^{18} g carbon would result in a 55 to 470 ppm drawdown of pCO_2 under Eocene conditions, indicating that the Arctic *Azolla* blooms may have had a significant effect on global atmospheric pCO_2 levels through enhanced burial of organic matter.

Received 26 September 2008; accepted 24 February 2009.

Corresponding author: E. N. Speelman. Tel.: +31 30 2536722; fax: +31 30 2535302; e-mail: e.speelman@geo.uu.nl

1. INTRODUCTION

Exceptionally high concentrations of intact microspore massulae and megaspores of the aquatic floating fern *Azolla* have been found in sediments recovered from the Lomonosov Ridge during Integrated Ocean Drilling Program (IODP) Expedition 302, indicating that this freshwater fern grew and reproduced *in situ* in the mid Eocene (~48.5 Ma) Arctic Ocean (Brinkhuis *et al.*, 2006; Moran *et al.*, 2006) (Fig. 1). Sporadically, mass abundances of *Azolla* remains have previously been recognized in the Eocene Arctic and Nordic Seas (e.g. Manum *et al.*, 1989; many confidential oil- and gas exploration studies; Eldrett *et al.*, 2004). Yet, concentrations of *Azolla* megaspores recovered at the Lomonosov Ridge Site are an order of magnitude higher than those found elsewhere (Brinkhuis *et al.*, 2006). Sustained growth of *Azolla* throughout the Arctic provides important constraints on the Eocene Arctic environment. The presence of the freshwater fern *Azolla*, both within the Arctic Basin and in all Nordic seas suggests that at least the surface waters were frequently fresh or brackish during the *Azolla* interval (Brinkhuis *et al.*, 2006). The occurrence of such a fresh surface layer in combination with

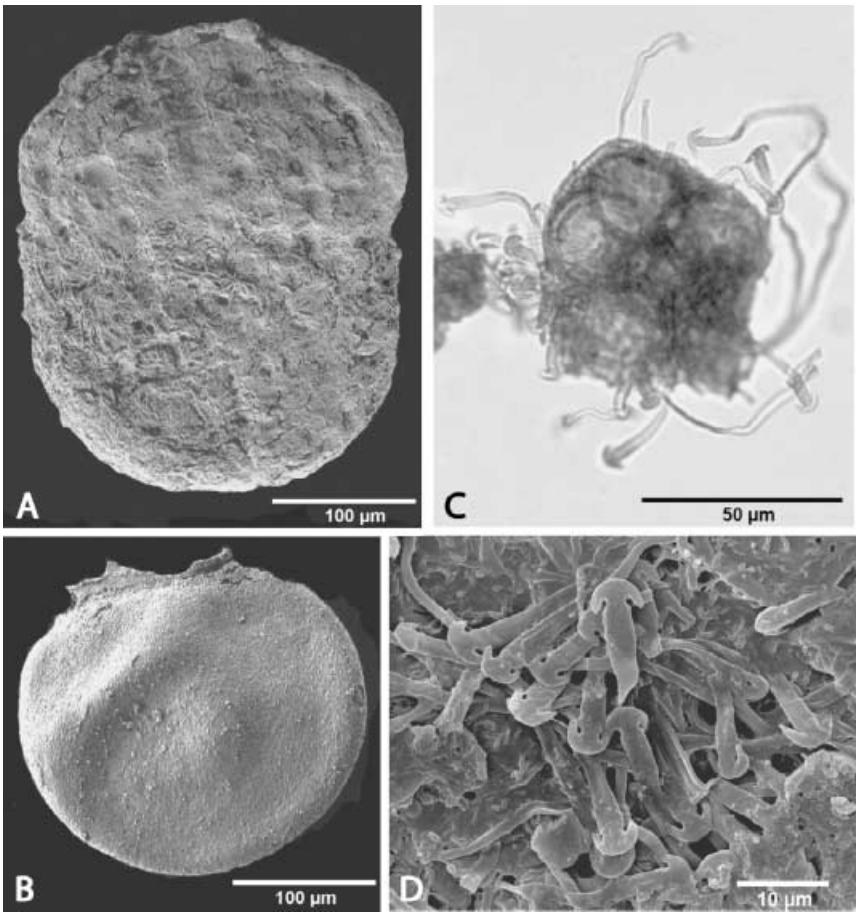

Fig. 1 Azolla mega- and microspores from Hole 302–4 A-11x (A) Scanning Electron Microscopy (SEM) image of megaspore apparatus showing the distal megaspore and the proximal float zone. (B). SEM image of dissected megaspore. (C) Light Microscopy (LM) image of microspore massulae showing the embedded microspores and fully developed glochidia. (D) SEM image of glochidia on microspore massulae showing anchor-shaped tips.

more saline deeper waters, as indicated by the presence of marine diatoms (Stickley *et al.*, 2008), suggests that the Eocene Arctic Basin was highly stratified. Salinity stratification, in combination with high riverine input of nutrients, and hence increased surface water productivity and the associated enhanced export of organic matter, are most likely responsible for the development of euxinic conditions in the lower part of the water column, comparable to the present-day Black Sea setting (Stein *et al.*, 2006). Interestingly, the *Azolla* phase approximately coincided with the onset of a global shift towards heavier deep sea benthic foraminifera $\delta^{13}C$ values (Zachos *et al.*, 2001) and an overall global cooling trend. In effect, around this time (~48.5 Ma) the transition from a global greenhouse climate towards the modern icehouse started (Tripati *et al.*, 2005; Zachos *et al.*, 2008), possibly heralded by decreasing atmospheric CO_2 concentrations (Pearson & Palmer, 2000; Pagani *et al.*, 2005). Together these notions suggest that sustained growth of *Azolla* in a major anoxic oceanic basin may have contributed substantially to decreasing atmospheric pCO_2-levels.

Here we discuss the potential role of *Azolla* as a modifier of nutrient cycles and evaluate if and how that role, in combination with the geological and oceanographical evolution of the Arctic Ocean, was instrumental for Earth's greenhouse to icehouse transition. We also present the first results from a multidisciplinary research project, combining results from microfossil assemblages, biomarker and geochemical analyses performed on sediments obtained from the Arctic Coring Expedition (ACEX) and *Azolla* cultivation experiments. The latter experiments were set up to elucidate the potential impact of elevated pCO_2 levels on the growth of *Azolla*. Results of these experiments are used to further constrain knowledge of *Azolla* growth rates, productivity and potential carbon drawdown in the context of reconstructed Eocene Arctic environmental conditions.

2. REVIEW OF EXISTING INFORMATION

2.1 Extant *Azolla*

Azolla is a genus of floating aquatic ferns with seven extant species, distributed throughout tropical and temperate regions (Saunders & Fowler, 1993). Extant *Azolla* ranks among the fastest growing plants on Earth, capable of fixing large amounts of carbon and producing vast amounts of organic nitrogen (Wagner, 1997). Dinitrogen fixing bacterial

symbionts are known to inhabit a special cavity within the dorsal leaf lobe of *Azolla*. These cyanobacteria, e.g. *Anabaena azollae*, fix atmospheric nitrogen and subsequently release it to *Azolla*, satisfying both its own requirement for combined nitrogen and that of its host. In exchange, the fern provides the endosymbiont with a protected environment and supplies it with a carbon source in the form of sucrose (Peters & Meeks, 1989). Through this symbiosis the aquatic fern *Azolla* is not limited by fixed nitrogen availability (Braun-Howland & Nierzwicki-Bauer, 1990) and under favourable conditions may outcompete other macrophytes, bloom fast, and form thick mats. Extant *Azolla* is known as a freshwater fern. Cultivation experiments with *Azolla filiculoides* show that *Azolla* grows well in water with maximum salinity levels of 2.5‰, but perishes when salinity is higher than 3.5‰ (van Kempen *et al.* unpublished results).

2.2 The Eocene Arctic setting

2.2.1 Paleoceanography and age assessment of the Azolla *interval*

The ACEX core was recovered from the Lomonosov Ridge, which is a fragment of continental crust that rifted from the Eurasian continental margin during the Late Palaeocene (~57 Ma ago) (Glebovsky *et al.*, 2006). In the late-middle Eocene, the Arctic Ocean was almost completely enclosed as the Norwegian Greenland Sea was not fully open yet (Scotese *et al.*, 1988). The, at that time, probably still shallow Fram Strait (Jakobsson *et al.*, 2007) possibly formed a deeper, intermittent, connection between the shallow Arctic Basin and the open ocean.

The age model for the ACEX core was established using biostratigraphical and cosmogenic isotope data, as usage of palaeomagnetic polarity data are problematic for this core (Backman *et al.*, 2008). In the Palaeogene, the dinoflagellate cysts (dinocysts) are abundant and occur fairly continuous throughout the record. Therefore, numerous dinocyst events could be calibrated against ODP Leg 151 Site 913B, located in the adjacent Norwegian-Greenland Sea, for which a good magnetostratigraphy is available (Eldrett *et al.*, 2004). Moreover, the *Azolla* horizon, being a widespread and well-calibrated acme event in the entire Arctic Basin and the adjacent Nordic Seas (Fig. 2), can also be used as a stratigraphic marker horizon itself (Brinkhuis *et al.*, 2006; Bujak, Brinkhuis, unpublished exploration data). Based on the observation that the Last Occurrence (LO) of *Azolla* for this interval coincides with the LO of *Eatonicysta ursulae* (Eldrett *et al.*, 2004), the top of the *Azolla* phase is dated at 48.1 Ma (magnetic polarity chronozone C21 r), based on Gradstein *et al.*, 2004). However, due to incomplete core recovery, the onset of the *Azolla* interval is missing in the ACEX core (Fig. 3). Also in Core 913B the *Azolla* interval is not fully represented as some spores, though in small numbers, are already present at the base of the core. So at this stage, only an estimate of the minimum duration of the entire *Azolla* interval can be given. In Core 913B *Azolla* is still present near or at the base of Chron 22n. Using the timescale by Gradstein *et al.* (2004), the beginning of the *Azolla* phase is dated at approximately 49.3 Ma, giving a total duration of 1.2 Ma for the entire *Azolla* interval.

2.2.2 Arctic Eocene environmental conditions

Vertebrate fauna recovered from Ellesmere Island in the 1970s provided some of the first evidence that temperatures in the early Eocene Arctic were substantially warmer than today. The discovery of early Eocene remains of a varanid lizard, the tortoise *Geochelone*, and the alligator *Allognathosuchus* suggested that winter temperatures rarely dipped below freezing (Estes & Hutchinson, 1980). Recently, Arctic sea surface temperatures (SSTs) have been estimated by applying the TEX_{86} index, an organic palaeothermometer that is independent of salinity (Schouten *et al.*, 2002; Powers *et al.*, 2004) and calibrated to mean annual SST. TEX_{86} values suggest SSTs of ~10 °C during, and 13–14 °C immediately following, the *Azolla* phase (Brinkhuis *et al.*, 2006). These values are similar to, or slightly higher than, other late Palaeocene and Eocene floral, faunal and isotopic proxy evidence for mean annual temperatures in the Arctic (Greenwood & Wing, 1995; Jahren & Sternberg, 2003). Stable oxygen isotope analyses of cellulose from middle Eocene *Metasequoia* wood at Axel Heiberg Island indicates that Arctic climate was not only warm (mean annual temperature of 13.2 ± 2.0 °C), but also quite humid, with an atmospheric water content approximately twice that of today (Jahren & Sternberg, 2003). Based on modern hydrology and fully coupled palaeoclimate simulations, it has been suggested that the warm greenhouse conditions characteristic of the Palaeogene period probably induced an intensified hydrological cycle with precipitation exceeding evaporation at high latitudes (Manabe, 1997; Huber *et al.*, 2003). Increased precipitation and reduced exchange of surface water between the Arctic and the open ocean would thus result in low salinity surface water in the Arctic.

Azolla megaspores, with or without attached microspore massulae and clusters of dispersed microspore massulae, were found in the ACEX sediments at abundances comparable to those documented in Palaeogene microlaminated freshwater pond facies (Collinson, 2002). The *in situ* growth and reproduction of *Azolla* in the Arctic Ocean, in combination with high abundances of chrysophyte cysts (the endogenously formed resting stage of these freshwater algae), indicate that fresh- or brackish waters frequently dominated the surface water layer (Stickley *et al.*, 2008). Based on qualitative data of endemic assemblages of marine diatoms and ebridians along with very high abundances of chrysophyte cysts, Stickley *et al.* (2008) confirmed the concomitant occurrence of lower surface water salinities and higher deeper water salinities, combined with episodic changes in salinity, stratification and thus trophic state. The, albeit incomplete, isolation of the Arctic from the worlds' oceans together with enhanced run-off may have

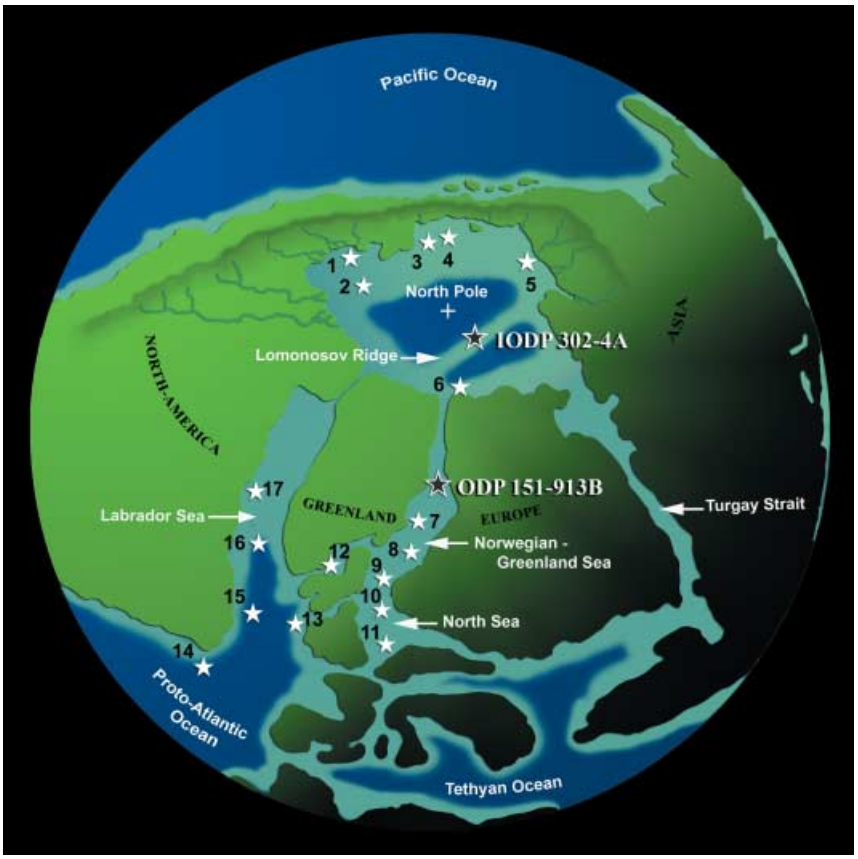

Fig. 2 Sites including the earliest middle Eocene *Azolla* acme in various regions of the Nordic Seas. Revision of Table S-1 and Figure S-3 in Brinkhuis *et al*., 2006 (supplementary information). Complementary sites are given in brackets. Region 1–2 Mackenzie Delta and Beaufort Basin; Region 3–4 North slop Alaska & Chukchi Sea (Crackerjack 1 OCS-Y-1320; Popcorn 1 OCS-Y-1275); Region 5 Siberian Shelf; Region 6 Barentsz Sea; Region 7–8 Norwegian–Greenland Sea (6302/6–16406/2–2, 6506/11–6, 6507/8–4, 6608/10–10, 6610/2–1 S, 7316/5–1, DSDP 343, ODP 643 A); Region 9–11 North Sea Basin (16/4–4, 24/12–1, 30/2–1, 34/4–2, M2/A02, M2Z/A02S1, M2Y/A02S2); Region 12 Faeroe-Shetland Basin; Region 13 Atlantic, Rockall Bank; Region 14 Grand Banks, Scotian Shelf; Region 15 Labrador, Hopedale Basin (South Labrador N-79); Region 16 Labrador, South Saglek Basin (Gilbert F-53); Region 17 Labrador, North Saglek Basin (Gjoa G-37, Hekja O-71, Ralegh N-18).

favoured development of anoxic conditions. Based on sediment lamination (Fig. 3), the absence of fossil benthic organisms, high concentrations of reduced sulphur (pyrite), and organic geochemical biomarker evidence, previous reports on the Arctic region concluded that bottom waters were at least temporally devoid of oxygen (Backman *et al.*, 2006; Brinkhuis *et al.*, 2006; Sluijs *et al.*, 2006; Stein *et al.*, 2006), also at the time of the *Azolla* interval. Considering the estimated duration of the *Azolla* phase (1.2 Ma), it is remarkable that the deeper saline waters did not become increasingly diluted over time to the point that it would be too fresh to sustain pyrite formation. The fact that it did not progressively freshened in itself provides evidence for the existence of a seaway connection. In turn, the resulting surface water stratification might have been a prerequisite for the development of massive *Azolla* occurrences. Given the found salinity intolerance of extant *Azolla* (van Kempen *et al.* unpublished results), admixing of much more saline water from greater depth would render the surface waters too saline for *Azolla*. In the ACEX sediments no intact vegetative *Azolla* material has been recovered (Brinkhuis *et al.*, 2006), indicating that most of the plant tissue was decomposed in the water column or at the sediment–water interface. High organic carbon fluxes, together with limited exchange with the atmosphere, partly related to the dense vegetation cover, usually renders water below *Azolla* mats dysoxic. If the presence of a floating mat of *Azolla* was a prerequisite for surface water stratification, mixing to some degree may have occurred during the long dark winter period. So at least during the growing season, the six months light period, a stratified water column existed with a strong halocline and anoxia at depth.

2.2.3 Atmospheric carbon dioxide levels

A reconstructed mean annual sea surface temperature of ~10 °C in the Eocene Arctic during the *Azolla* phase prevailed in absence of oceanic heat transport (Brinkhuis *et al.*, 2006). This implies that increased greenhouse gas concentrations and associated feedbacks must have been the dominant factor in keeping high latitudes warm (Huber *et al.*, 2003). Changes in the carbon dioxide concentrations in the atmosphere are commonly regarded as likely forcing mechanism of global climate on geological time scales because of the large and predictable effect of CO_2 on temperature (Pearson & Palmer, 2000). The exact relation between atmospheric CO_2 concentration and the greenhouse climate of the early Eocene is uncertain because proxy measurements from palaeosols (Royer *et al.*, 2001; Yapp, 2004), marine boron isotopes (Pearson & Palmer, 2000) and leaf stomatal indices (Royer *et al.*, 2001) give extremely variable estimates of atmospheric

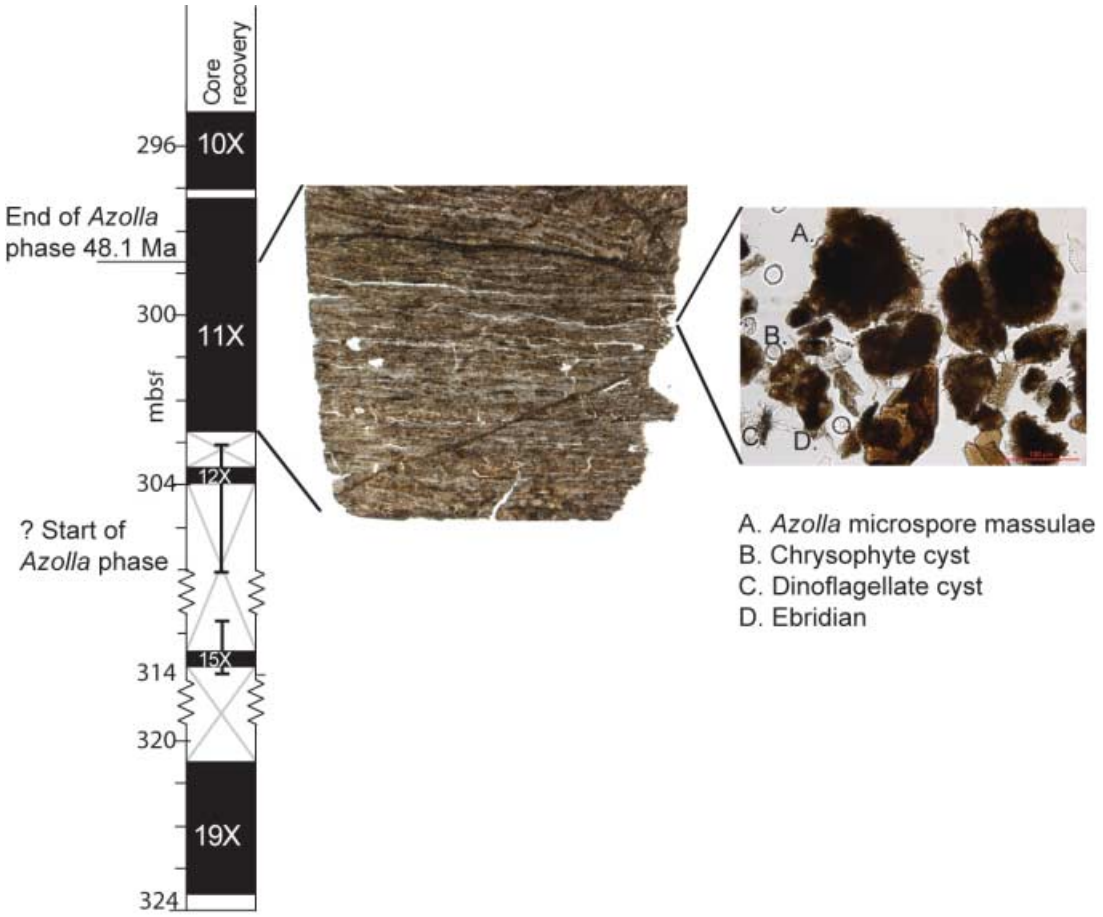

Fig. 3 ACEX core recovery. Close up of laminated sediment (courtesy of M. Collinson) and image of fossil content, showing *Azolla* microspore massulae, chrysophyte cysts, dinoflagellates and ebridians.

CO_2 concentrations between 400 and 3500 ppmv. In the middle Eocene pCO_2 is assumed to have been up to 10 times preindustrial values (Pearson & Palmer, 2000). It is well known that high pCO_2 may stimulate growth of *Azolla* species (Allen *et al.*, 1988; Idso *et al.*, 1989; Koizumi *et al.*, 2001). Moreover, there are indications that at higher CO_2 concentrations plants generally cope better with environmental stresses such as high salinity levels (Reuveni *et al.*, 1997).

The *Azolla* phase in the Eocene Arctic, during which the organic carbon content of the sediment reaches a maximum (Moran *et al.*, 2006), coincides with a global shift towards heavier $\delta^{13}C$ values in benthic foraminifera (e.g. Zachos *et al.*, 2001), suggesting enhanced global sequestration of organic matter. Waddell & Moore (2008) also found a positive $\delta^{13}C$ excursion in fish bone remains and speculated that during a period of extreme primary productivity the Arctic surface waters became depleted in ^{12}C, which subsequently resulted in burial of the fish bones with ^{13}C enriched organic matter. The combination of extremely high primary production by *Azolla* on a freshwater surface, together with the anoxic and saline nature of Eocene Arctic deep waters, makes the Arctic Basin ideally suited as an important carbon sink. Sustained growth of *Azolla* in a major anoxic oceanic basin may have contributed significantly to reducing atmospheric CO_2 levels, either directly by the storage of large amounts of organic carbon or/and indirectly through enhanced nitrogen fixation. Nitrogen-fixing bacteria play a key role in global biogeochemical cycles as availability of fixed nitrogen and dissolved phosphorus together limit primary productivity and thus CO_2 fixation. In anoxic environments a substantial loss of fixed nitrogen occurs through denitrification or anaerobic ammonia oxidation activity (Kuypers *et al.*, 2003) and on shorter timescales fixed nitrogen is often a limiting nutrient. During growth of *Azolla*, however, this loss of fixed nitrogen may be compensated by symbiotic nitrogen-fixating bacteria.

3. MATERIALS AND METHODS

3.1 Sample material: extant *Azolla*

Azolla filiculoides was collected from an arable land ditch in the surroundings of Elst, the Netherlands (N51°55′48″;

E5°50′6″). Two fresh *Azolla* samples were used for biomarker and compound-specific isotope analysis. Bulk *Azolla* and manually picked megaspores were analysed for their $\delta^{13}C$ and $\delta^{15}N$ isotopic composition.

3.2 Sample material: IODP 302 (ACEX) sediments

During the IODP 302 ACEX expedition, cores were taken at 1288 m water depth at the Lomonosov Ridge, Expedition 302, Hole M0004A, 87.87°N, 136.18°E (Backman *et al.*, 2006). In this study we used sediments from lithological Unit 2, Core M0004A-11 × 297.31 to 302.63 mbsf covering the *Azolla* interval as encountered in the core (Brinkhuis *et al.*, 2006). This unit is dominated by very dark clay mud-bearing biosiliceous ooze. Palaeowater depths are estimated to be shallow, perhaps on the order of ~200 m (Moran *et al.*, 2006). The entire core 11X has pale-grey dark-grey laminations. The *Azolla* remains are associated with the light layer in the scanning electron microscopy (SEM) pictures (Brinkhuis *et al.*, 2006). The recovery within section 11X was good, including the end of the *Azolla* interval. Fifty-four samples were used for palynological analyses, giving a sample resolution of one sample every 10 cm. In total, 90 samples were used for bulk geochemical analyses and two for biomarker and compound-specific isotope analyses. *Azolla* megaspores from the ACEX core were manually picked for the determination of $\delta^{13}C$ values.

3.3 Pilot experiment: Growth of *Azolla* at elevated atmospheric CO_2 concentrations

To study the influence of different atmospheric carbon dioxide concentrations on *Azolla* growth, *Azolla filiculoides* was grown in glass aquaria with a water volume of 15.6 L and headspace of 3.4 L. The aquaria were made air-tight except for a gas overflow outlet. The aquaria were placed in a water bath with a controlled mean temperature of 15 °C. At the start of the experiment 4 g of fresh *Azolla* was introduced in each aquarium. Three different treatments with specific atmospheric CO_2 concentrations were completed, with eight replicates per treatment (Fig. 4). At the start of the experiments the measured CO_2 concentrations in the headspaces of the different aquaria amounted to 340, 760 and 1910 ppm, respectively. Appropriate atmospheric CO_2 concentrations were attained by mixing compressed air with custom-made mixtures of various concentrations of CO_2 in synthetic air (Air Liquide, Eindhoven, the Netherlands), using mass flow controllers and gas blenders (Bronkhorst Hi-Tec, Veenendaal, the Netherlands). Per treatment the gas mixture was uniformly distributed between the headspaces of the eight aquaria, refreshing the air volume within each aquarium every 5 min. The nutrient solution in the aquaria contained 1.75 mmol L^{-1} $NaHCO_3$, 1.75 mmol L^{-1} $CaCl_2 \cdot 2H_2O$, 0.025 mmol L^{-1} $NaH_2PO \cdot H_2O$, 1 mmol L^{-1} K_2SO_4, 1 mmol L^{-1} $MgSO_4 \cdot 7H_2O$, 0.01 mmol L^{-1} Fe-EDTA, 0.001 mmol L^{-1} $CuSO_4 \cdot 5H_2O$, 0.02 mmol L^{-1} $MnCl_2 \cdot 4H_2O$, 0.01 mmol L^{-1} $ZnSO_4 \cdot 7H_2O$, 0.003 mmol L^{-1} $Na_2MoO_4 \cdot 2H_2O$, 0.02 mmol L^{-1} H_3BO_3 and 0.004 mmol L^{-1} $CoCl_2 \cdot 6H_2O$ and was adjusted to a pH of 7.5 using 30% HCl. Fresh nutrient solution was supplied at a rate of 0.2 L h^{-1} from containers using peristaltic pumps, the water level being held at a constant level by means of an overflow outlet (Fig. 4). Since no nitrogen was added to the nutrient solution, *Azolla* completely depend on its cyanobacterial symbionts for nitrogen supply. The experiments were performed in a greenhouse where the light flux amounted to at least 150 μmol m^{-1} s^{-1} at vegetation level, supplemented by 600 watt HDN lamps set to a day : night rhythm of 16 : 8 hours.

Fig. 4 The experimental set up in the greenhouse.

The CO_2 concentrations in the headspaces above each aquarium were monitored. Air samples were taken with a syringe at the gas overflow outlet and CO_2 concentrations were measured directly using an Infrared Gas Analyzer (IRGA, type ABB Advance Optima, Ettenleur, The Netherlands). Nutrient solutions of all aquaria were sampled weekly for nutrient analyses with the aid of rhizons. The solutions were analysed for pH, total inorganic carbon (TIC) using an Infrared Gas

Analyzer (IRGA, type ABB Advance Optima), and total concentrations of Al, Ca, Fe, K, Mg, Mn, Na, P, S, Si and Zn using inductively coupled plasma emission spectrometry (ICP-OES). To avoid contamination all used glassware was immersed in acid (30% HCl) for 24 h after which it was rinsed three times with demineralized water. Total inorganic carbon content in the nutrient solution was measured by injection of 0.2 mL of the nutrient solution into a concentrated H_2PO_4 solution of 2.1% in a glass reservoir that was directly coupled to an infrared gas analyser to ensure direct measurement of released dissolved carbon. Plants were harvested on day 0, 10, 17 and 23. At harvest total fresh weight of the *Azolla* was determined for each aquarium after which 4 g of fresh *Azolla* was put back into the aquaria while the rest was dried at 70 °C for 48 h to determine the element composition of the biomass. The total dry weight at a specific sampling time was calculated using the dry weight to fresh weight ratio from the subsample. Cumulative dry weights were based on using these dry weight ratios, adding them up to the total dry weight calculated for the previous time intervals. To analyse nutrient contents of plant tissue, dried samples were ground in liquid nitrogen. Nitrogen and carbon were subsequently measured with a CNS analyzer (type Fisons NA1500). Two hundred micrograms plant material was digested using a acid mixture (4 mL HNO_3 (65%) and 1 mL H_2O_2 (30%)) (Kingston & Haswell, 1997) in Teflon vessels heated in a Milestone microwave oven (type mls 1200 mega, Sorisole, Italy). Total concentrations of Al, Ca, Fe, K, Mg, Mn, Na, P, S, Si, and Zn were measured in diluted digestates.

3.4 Palynology

Subsamples were first cleaned by removing the top part and oven dried at 60 °C overnight. Agepon (Agfa-Gevaert, art Nr AKX2P, Leverkusen Germany) wetting agent was added. Precisely weighted sediment samples were then treated with HCl and HF in standard palynological treatment. Residues were sieved retaining the fraction size between 15 and 250 µm. *Lycopodium clavatum* tablets containing a known amount of spores were added to the samples to calculate the concentrations of *Azolla* massulae per gram of sediment. The samples were then examined under a binocular microscope at a magnification of ×400.

3.5 Bulk TOC, N, S, and isotope measurements

Extant *Azolla* samples were oven dried at 70 °C for 24 h. Total organic carbon (TOC), $\delta^{13}C_{TOC}$, total nitrogen content (N_{tot}) and bulk $\delta^{15}N$ were measured using an elemental analyser (Fison NA 1500 CNS), connected to a mass spectrometer (Finnigan Delta Plus). $\delta^{13}C_{TOC}$ values are reported against Vienna Peedee Belemnite (VPDB). $\delta^{15}N$ values are calculated as per mille excess above their natural abundance in air. Analytical precision and accuracy were determined by replicate analyses and by comparison with international and in-house standards. Precision was better than 0.1% for TOC, N_{tot}, and $\delta^{13}C_{TOC}$ and 0.15‰ $\delta^{15}N$.

3.6 Sediment bulk TOC, N, S, and isotope measurements

TOC, N_{tot}, total nitrogen isotopic composition ($\delta^{15}N$) and total sulphur content of bulk sediment samples were determined, with a sampling spacing of 10 cm for the *Azolla* interval. All sediment samples were freeze-dried and subsequently grounded in an agate mortar. Prior to the determination of organic carbon content and $\delta^{13}C_{TOC}$ inorganic carbon was removed. Samples were treated with 10% HCl, rinsed with demineralized water to remove $CaCl_2$, and dried. TOC, $\delta^{13}C_{TOC}$, N_{tot} and $\delta^{15}N$ were measured using the same procedure, with similar precision and accuracy, as described above in section 3.5. Total concentrations of S were determined after digestion in a mixture of HF, HNO_3, and $HClO_4$ and final solution in 1 M HCl via ICP-OES (PerkinElmer Optima 3000, PerkinElmer, Waltham, MA, USA). The accuracy and precision of the measurements were monitored by including international and laboratory standards and were better than 3%.

3.7 Compound-specific isotope analyses ACEX sediments and extant *Azolla*

Both ACEX sediments and extant *Azolla* specimens were freeze-dried, powdered and subsequently extracted with an Accelerated Solvent Extractor (Dionex, Sunnyvale, CA, USA) using a dichloromethane (DCM)–methanol (MeOH) mixture (9 : 1, v/v). To separate the compounds of interest an aliquot (*c.* 15 mg) of the total extract was methylated with BF_3/MeOH at 60 °C for 10 min and subsequently separated by preparative thin layer chromatography (TLC) on kieselgel 60 (0.25 mm, Merck, Darmstadt, Germany) as described by Skipski *et al.* (1965). The lower, more polar, bands were silylated with BSTFA in pyridine to convert the alcohols into the corresponding TMS-ethers. Components were identified by GC/MS (Thermo Trace GC Ultra, Thermo Fisher Scientific Inc.). Samples were on-column injected at 70 °C, on a CP-Sil 5CB fused silica column (30 m × 0.32 mm i.d., film thickness 0.1 µm) with helium as carrier gas set at constant pressure (100 KPa). The oven was programmed to 130 °C at 20 °C min^{-1} and then to 320 °C at 4 °C min^{-1}, followed by an isothermal hold for 20 min. Compound-specific $\delta^{13}C$ values were determined using isotope ratio monitoring gas chromatography-mass spectrometry (GC-IRMS), using a ThermoFinnigan Delta-Plus XP mass spectrometer. A similar column and oven program were used as described above, though with a constant flow of 1.2 mL min^{-1}. Co-injected squalane, with a known, offline determined, isotopic composition was used as internal standard. Carbon isotopic compositions are reported relative to the VPDB standard and are based on duplicate analyses of well-resolved peaks and represent averaged values. In the case of alcohol moieties, the $\delta^{13}C$ value of the BSTFA used for silylation

was determined by derivatization of an authentic alcohol (myo-inositol) standard with a known $\delta^{13}C$ composition.

Standard deviation of co-injected squalane was 0.2‰. Duplicates had a standard deviation better than 0.5‰.

4. RESULTS AND DISCUSSION

In order to further constrain the exact environmental conditions facilitating the Eocene Arctic *Azolla* blooms a suite of geochemical and palynological analyses are performed. Furthermore, the influence of these Eocene conditions is investigated using *Azolla* cultivation experiments, focusing on elevated pCO_2 conditions. Finally, the combined results will shed light on *Azolla* occurrence, productivity and potential atmospheric CO_2 drawdown.

4.1 Pilot cultivation experiments with extant *Azolla*: a key to the past

During the middle Eocene atmospheric CO_2 levels were much higher than today (Pearson & Palmer, 2000). To investigate the influence of elevated atmospheric CO_2 concentrations on *Azolla* growth rates, CO_2 concentrations in the headspaces of the cultivation aquaria were set to values of 340 ppm (control), 760 ppm and 1910 ppm, respectively. Distinct increases in biomass production in response to elevated carbon dioxide concentrations were evident (Fig. 5). After 23 days the total dry biomass amounted to 3.92 ± 0.37, 5.98 ± 0.47 and 7.87 ± 1.04, respectively. The amount of biomass produced in the high (1910 ppm) CO_2 treatment was twice that of the biomass produced in the control treatment at 340 ppm. The experiment using an intermediate CO_2 concentration (760 ppm) yielded 1.5 times more biomass (Fig. 5). During growth in the light period (16 h day^{-1}) the preset CO_2 concentrations within the headspaces dropped appreciably. Lowest CO_2 concentrations in headspaces were measured just before harvest, when *Azolla* densities were highest, during the light period. On average pCO_2 values dropped from their preset concentrations to values of 170 ± 100 ppm, 330 ± 140 ppm, and 1080 ± 190 ppm, respectively. Flushing the headspaces every 5 min thus did not suffice to maintain constant pCO_2 levels. Both pH (7.53 ± 0.27, 7.47 ± 0.17 and 7.43 ± 0.18 in the treatments with 340, 760 and 1910 ppm atmospheric CO_2, respectively) and TIC (819 ± 76, 857 ± 94 and 800 ± 175 in the respective treatments) of the culture medium remained constant throughout the experiment with no differences at different levels of CO_2 concentrations. Given the low diffusion rate of CO_2 into water (0.21 m day^{-1} or 2.4 μm s^{-1}) (Zeebe & Wolf-Gladrow, 2001) and the observed stability of pH and TIC in the culture medium, the rapid decreasing CO_2 concentrations in headspace can only be attributed to high CO_2 (g) uptake rates of *Azolla*.

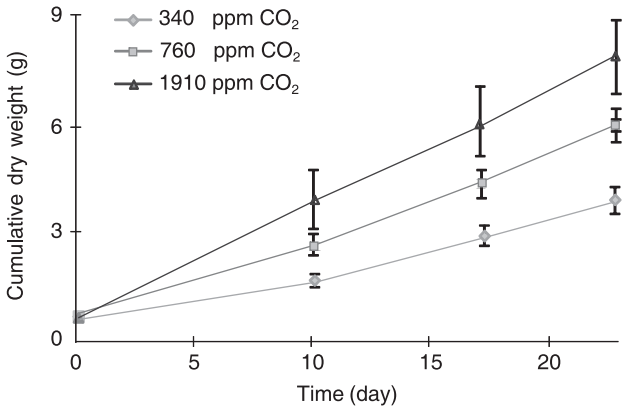

Fig. 5 Plot of cumulative biomass against time for different pCO_2 conditions. Cumulative biomass was calculated by using the fresh weight/dry weight ratio of the subsamples that were taken each harvest for dry weight measurements. Using this ratio the total biomass per week was calculated and this was added to the total dry weight of the week before.

Analyses of the chemical composition of the culture medium showed that the supply rate of fresh medium of 0.2 L h^{-1} was not high enough to keep the phosphorus concentration at a constant level (P concentrations dropped from 20 μmol L^{-1} to 6 μmol L^{-1}). The concentrations of the other elements in the culture medium remained constant The measured nutrient concentrations in *Azolla* all fall within the range of average concentrations of mineral nutrients in plant dry material matter (Marschner, 1995). The decreasing nutrient and N concentrations probably reflect diluting effects. Given the preserved linear growth rates during the experiments (Fig. 5), this dilution did not adversely influence *Azolla* biomass production.

These experiments indicate that at elevated CO_2 (g) concentrations the carbon dioxide uptake of *Azolla filiculoides* increases and that biomass is produced at higher rates, suggesting that CO_2 might be a limiting factor for *Azolla* growth. Hence, *Azolla* could potentially grow at significantly higher rates under the elevated Eocene pCO_2 conditions than under present-day circumstances. However, it should be noted that other environmental conditions like salinity (Rai *et al.*, 2001), pH (Moretti & Gigliano, 1988; Cary & Weerts, 1992) or nutrient availability (Sah *et al.*, 1989) also affect *Azolla* biomass production.

4.2 Sedimentary signals of the Eocene Arctic *Azolla* bloom

4.2.1 Bulk parameters of ACEX sediments

Our high-resolution ACEX TOC profile reveals values ranging between 3.1 and 6.0 wt% (Fig. 6). After the *Azolla* phase (above 289.7 mbsf) TOC decreased to lower levels, around 2 wt%. The high-resolution record of *Azolla* massulae counts (Fig. 6) confirms the cyclic nature of the abundance pattern in the *Azolla* record as previously described in Brinkhuis *et al.* (2006). These cycles have a spacing of just over 1 m and are positively correlated with the TOC content (Fig. 6). Sangiorgi *et al.* (2008) applied a Blackman–Tuckey power spectral

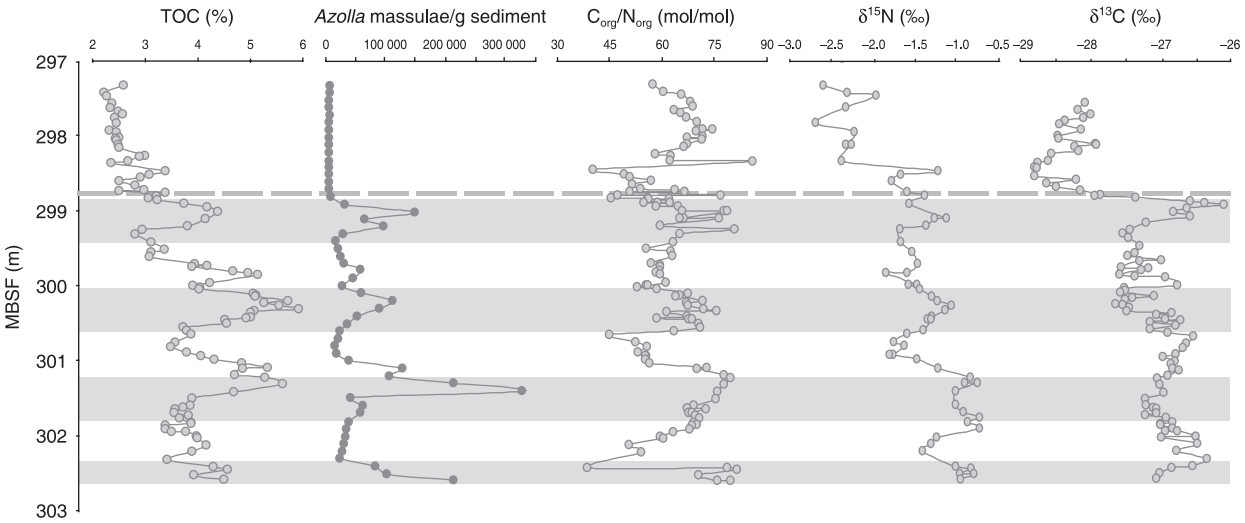

Fig. 6 Palynological and geochemical data of high resolution analyses of ACEX sediment, including *Azolla* massulae counts, total organic carbon (TOC) (%), $\delta^{13}C_{TOC}$ (‰), $\delta^{15}N$ (‰) and C_{org}/N_{org} ratio.

analysis to palynological and siliceous microfossil data for the middle Eocene (~46 Ma) core section between ~236 to 241 mcd (metres composite depth) and also found a 1 m periodicity. The available age model for the ACEX core (Backman *et al.*, 2008), and the derived sedimentation rate of 24.3 m Ma^{-1} during the middle Eocene (~46 Ma), suggest that the 1 m cyclicity is compatible with a Milankovitch-type orbital forcing, representing obliquity. Based on the high latitudinal setting, an obliquity signal is expected to be present. However, since for the *Azolla* phase the age model suggests an overall sedimentation rate of 12.7 m Ma^{-1} (Backman *et al.*, 2008), the 1 m cyclicity would correspond to ~80 000 years. Yet, given that the onset of *Azolla* is missing due to failure in core recovery (Fig. 3), it could be possible that the observed cyclicity in the *Azolla* record still represents obliquity. If these cycles indeed respond to obliquity the amount of time included in the entire *Azolla* event, represented in the recovered sections of the ACEX core, can be calculated. Based on the observed four obliquity cycles within the recovered part from the *Azolla* interval in the ACEX core (Fig. 6), the estimated minimum duration is 160 kyr. The recovered *Azolla* interval in the ACEX core thus represents 160 kyr, with a 24.3-m Ma^{-1} sedimentation rate. The duration of the entire *Azolla* interval of 1.2 Ma can be inferred from dating of the *Azolla* phase in ODP Leg 151 Hole 913B (Eldrett *et al.*, 2004) (with a 12.7-m Ma^{-1} sedimentation rate based on the overall age model (Backman *et al.*, 2008)), assuming that the Azolla phase also covered part of the unrecovered core material.

Sulphur concentrations are high throughout the interval, varying between 47 and 72 mg g^{-1} dry sediment. C/S ratios show an atomic C_{org}/S ratio of 1–2 during and after the *Azolla* interval (Fig. 7A). The correlation between Fe and S indicates that most of the S is present in the form of pyrite (Fig. 7B). The black dots represent samples from the *Azolla* interval and all plots above the pyrite line (excess S). This indicates that S must be present as greigite or organically bound S as well. The four points in grey plotting below the pyrite line represent samples from after the *Azolla* interval (above 298.8 mbsf). The accumulation of large quantities of organic matter in an euxinic environment is consistent with the findings of Kurtz *et al.* (2003) who showed a global minimum in C_{org}/S pyrite (C_{org}/S ratio of 2–4) during the early Eocene. The presence of sulphate-rich waters in the deeper parts of the Arctic Basin provides additional evidence for the salinity stratification of the basin described above.

In view of the inferred marine setting of the site during the Eocene, an extensive riverine influx of fixed nitrogen seems unlikely. Regeneration or atmospheric nitrogen fixation, therefore, must have played a major role in nitrogen supply. Bulk sedimentary nitrogen isotope ratios are persistently low, between –0.7 and –2.4‰ throughout the *Azolla* phase (Fig. 6) and drop to even lower values (<–2‰) afterwards. Variations in $\delta^{15}N$ in surface sediments generally reflect differences in relative nutrient utilization (Schubert *et al.*, 2001) and denitrification or anammox (Altabet & Francois, 1994; Montoya *et al.*, 2004), but can also be influenced by exchange with open-ocean water or runoff. Under oxygen-depleted conditions, the reduction of nitrate leads to enrichment of the residual nitrate in ^{15}N relative to the mean value because $^{14}NO_3$ is more readily reduced by bacteria. Under the prevailing anoxic conditions in the Eocene Arctic relatively enriched ^{15}N values are thus expected as upwelling of nitrate-deficit waters generated in the dysoxic deeper parts of the water column by denitrification or anammox bacteria (Cline & Kaplan, 1975; Kuypers *et al.*, 2003) followed by Redfield-type nutrient

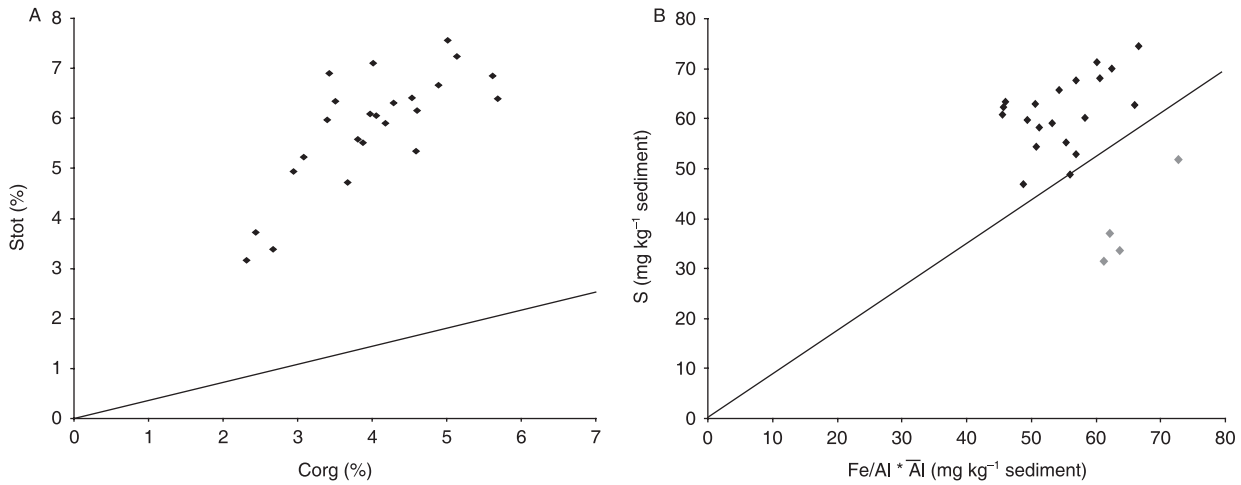

Fig. 7 (A) Plot of weight percentage organic carbon (wt%) vs. weight percentage total sulphur concentration (wt%). The black line indicates the modern normal marine (non-euxinic) sediments (Berner, 1984), (B) Fe normalized over aluminum concentration (mg/kg sediment) vs. total sulphur content (mg/kg sediment). The S/Fe weight ratio of pyrite (1.15) is plotted. Black dots represent samples from the *Azolla* interval, grey dots represent samples from after the interval.

drawdown should result in nitrate limitation in the photic zone, which would result in a positive ^{15}N excursion. The small and constant offset (mean 0.9‰) between the $\delta^{15}N_{tot}$ and $\delta^{15}N_{org}$ found earlier by Knies *et al.* (2008) confirms that there is little net influence of NH_4^+ generation or vertical diffusion on the sedimentary ^{15}N values. Hence we use bulk $\delta^{15}N$ values for reconstruction of the marine nitrogen cycle. The low $\delta^{15}N$ values encountered in the Arctic sediments point towards the presence of N_2-fixing organisms, which are present in extant *Azolla* species as symbionts. The cultured *Azolla filiculoides* biomass had a similarly low average $\delta^{15}N$ of –1.5‰, also consistent with ^{15}N values reported for other biomass produced by N_2 fixation (between –1‰ and –2‰) (Minagawa & Wada, 1986; Kuypers *et al.*, 2004). Whereas the oxygen-depleted water condition resulted in the large scale loss of biologically available nitrogen, phosphorus might have been regenerated more efficiently under such conditions (Gächter *et al.*, 1988; Van Cappellen & Ingall, 1994). Organisms with nitrogen-fixating symbionts, like *Azolla*, would have had an ecological advantage. However, direct evidence for the presence of *Anabaena azollae* or other symbiotic nitrogen-fixing cyanobacteria in the Eocene Arctic, either in the form of biomarkers or morphological evidence, has not been found yet.

In extant *Azolla* C/N ratios vary between 9 and 15. C_{org}/N_{tot} ratios in the ACEX core were adjusted for the contribution of inorganic nitrogen by subtracting a fixed amount of inorganic nitrogen (47 μmol g^{-1}). This amount is based on extrapolation of the linear relation between C_{org} and N_{tot} content. This concentration is similar to the amount used for subtraction as determined by Knies *et al.* (2008) using $\delta^{15}N$ values. The C_{org}/N_{tot} ratios in the ACEX sediments vary from 27 to 46. The calculated C_{org}/N_{org} ratios vary from 40 to 80 (Fig. 6) and are significantly higher than those of extant *Azolla*. These higher C_{org}/N_{org} ratios point towards extensive selective degradation of nitrogen-rich organic compounds (e.g. amino acids), despite the continuous anoxic bottom waters as evidenced by the presence of laminations in the sediment. After each *Azolla* megaspore abundance peak, a marked decrease in C/N ratio can be observed, which coincides with a drop in $\delta^{15}N$ (Fig. 6). Changes in C/N ratios, therefore, could be linked to changes in source organisms (*Azolla* vs. marine plankton) or changes in N preservation. Compositional changes, on the other hand, are not reflected in the observed bulk ^{13}C values, which vary around –27.7‰ throughout the interval (Fig. 6). The decrease in $\delta^{15}N$ probably indicates that after periods of extensive *Azolla* growth, the water column became slightly more oxygenated, decreasing the impact of denitrification/anammox until the next *Azolla* bloom.

4.2.2 Compound-specific isotope analyses

In addition to the existing palynological data, a recent study provided molecular evidence for the pervasive past presence of *Azolla* in a freshwater Eocene Arctic setting (Speelman *et al.*, 2009). It was shown that the total lipid fraction of extant *Azolla* ferns contains a series of mid-chain ω20 alkanols, 1,ω20 diols and ω20 hydroxy fatty acids with carbon chain lengths ranging from C_{27}–C_{36}. Selective extraction of extant *Azolla* leaf surface lipids revealed that these compounds most likely originate from *Azolla* leaf waxes. The ACEX sediments from the *Azolla* interval contained most of the described ω20 compounds. Especially relatively high quantities of compounds identified as 1,ω20 C_{30}–C_{36} diols were detected in both extant *Azolla* species and in sediments from the ACEX core. Based on the uniqueness of the ω20 hydroxy compound series and their relative stability, these compounds can be considered to be excellent biomarkers for *Azolla*, can thus be used for compound-specific isotope ($\delta^{13}C$) analyses, and therefore serve as palaeo-environmental indicators for *Azolla*.

Table 1 $\delta^{13}C$ compound-specific isotopes (‰ vs. VPDB) for selected compounds and $\delta^{13}C$ for bulk organic matter and manually picked *Azolla* megaspores encountered in extant *Azolla* and ACEX sediment extracts

Diols extant *Azolla*	$\delta^{13}C$ (‰)	Diols ACEX	$\delta^{13}C$ (‰)	Extant *Azolla*	$\delta^{13}C$ (‰)	ACEX	$\delta^{13}C$ (‰)
1,11 C_{30} diol	–39.1	1,11 C_{30} diol	–	β-sitosterol	–32.6	β-sitosterol	–29.1
1,13 C_{32} diol	–38.0	1,13 C_{32} diol	–30.1	$\delta^{13}C_{TOC}$	–30.3	$\delta^{13}C_{TOC}$	–27.6
1,15 C_{34} diol	–38.7	1,15 C_{34} diol	–31.3	Megaspores	–30.5	Megaspores	–27.7
1,17 C_{36} diol	–39.9	1,17 C_{36} diol	–29.7				

Compound-specific $\delta^{13}C$ values can provide insight into Eocene $\delta^{13}CO_2$. As β-sitosterol is the most abundant sterol present in extracts from *Azolla* (Speelman *et al.*, 2009), the ^{13}C of β-sitosterol was measured both for extant *Azolla* and for ACEX sediments (Table 1). Here we compare stable carbon isotopic compositions of TOC, spores and specific biomarkers of extant *Azolla* and ACEX sediments from the *Azolla* phase to gain insight into differences in the present-day and Eocene environmental conditions at which *Azolla* fixed carbon.

Bulk $\delta^{13}C$ values for recent *Azolla* of ~–30 ‰ (Table 1) are consistent with the findings by Bunn & Boon (1993) for ferns (Pterophyta) in general and in line with their use of the C3 pathway of carbon fixation (Hayes, 2001). The $\delta^{13}C$ of the megaspores of extant *Azolla* is also ~–30‰, indicating that there is no significant difference in ^{13}C content between *Azolla* biomass and spores. However, the $\delta^{13}C$ ratios of the lipids extracted from *Azolla* are substantially depleted: the 1,ω20 C_{30}–C_{36} diols have $\delta^{13}C$ values of –38.0 to –39.9‰ and the $\delta^{13}C$ values for β-sitosterol is –32.6‰ (Speelman *et al.*, 2009). Such differences are generally observed in biomass (Hayes, 2001) and lipids are typically 4–8‰ depleted in ^{13}C values relative to total cell material. The TOC and the *Azolla* megaspores contain isotopically heavy sugars and proteins and, therefore, their $\delta^{13}C$ values are higher than those of the individual lipids. The difference in $\delta^{13}C$ values between the β-sitosterol and the diols is *c.* 6.5‰. Differences in the biosynthetic pathways of isoprenoids (including β-sitosterol) and the compounds with straight chain carbon skeletons (i.e. ω20 diols) will influence the ^{13}C composition of the individual compounds. These differences may, possibly as a result of the alternative pyruvate/glyeraldehyde-3-phosphate pathway, differ by up to 8‰ (Schouten *et al.*, 1998), which is sufficient to explain the observed 6.5‰ difference between the isoprenoid β-sitosterol and the straight chain ω20 diols in extant *Azolla*.

Of all measured parameters (Table 1) the $\delta^{13}C$ values of the diols probably give the most reliable insight into differences in the present-day and Eocene environmental conditions at which *Azolla* fixed carbon. The *Azolla*-specific diols in the ACEX sediments show an enrichment of at least 8‰ relative to values observed in extant *Azolla*, between –29.7 to –31.3‰ (Table 1). β-sitosterol is also enriched in ^{13}C in the Eocene material but only by ~3‰, a similar enrichment as observed for $\delta^{13}C_{TOC}$ and $\delta^{13}C$ of the megaspores (Table 1). The difference between the β-sitosterol and the ω20 diols is only ~1‰ in the sediment instead of 6.5‰ in extant *Azolla*. This could be due to a mixed origin for the Eocene β-sitosterol. This sterol is not specific for *Azolla* and is probably also produced by algae growing in the water column in the Eocene Arctic, producing β-sitosterol with a different ^{13}C content. Alternatively, the different offsets could be explained by a difference in biosynthetic pathways between Eocene *Azolla* and extant *Azolla*, resulting in a much smaller difference between isoprenoidal and acetogenic lipids. Based on the similarity of the distribution of the ω20 diols in extant and Eocene *Azolla* this seems unlikely. Sedimentary TOC does not solely contain *Azolla* remains so it also represents mixed contributions. The difference between the $\delta^{13}C$ values of the extant and Eocene *Azolla* megaspores is also only 3‰. This could be caused by diagenesis. Extant *Azolla* megaspores still contain a shell mainly consisting of both sugars and protein components, which are typically substantially enriched in $\delta^{13}C$ (Hayes, 2001). During diagenesis, sugar and protein carbon degrades more easily, leaving the megaspores increasingly isotopically depleted. The $\delta^{13}C$ values of the *Azolla*-specific ω20 diols indicate the largest and probably most accurate difference (8‰) in isotopic composition between the present and the Eocene.

Based on reconstructions of Eocene atmospheric pCO_2 levels, suggesting higher concentrations, and the observation that *Azolla* also takes up atmospheric CO_2, and grows faster at elevated pCO_2 levels, at first sight, lighter rather than heavier $\delta^{13}C$ values (Hayes *et al.*, 1999) for *Azolla* biomarkers in ACEX sediment compared to extant *Azolla* are expected. Additionally, the cultured *Azolla* does not seem to fractionate to the full extent during carbon fixation (i.e. bulk values of *c.* –33‰ would be expected). $\delta^{13}C$ of atmospheric CO_2 taken up by *Azolla* was probably different in the Eocene and could thus also influence the $\delta^{13}C$ ratios. In fact, based on $\delta^{13}C$ analyses on foraminifera, the atmospheric CO_2 $\delta^{13}C$ was 3‰ enriched in the Eocene relative to the present-day atmospheric CO_2 $\delta^{13}C$ (Hayes *et al.*, 1999; Pearson *et al.*, 2001; Zachos *et al.*, 2001). A similar enrichment of Eocene *Azolla* biomass and lipids would be expected if they would grow under identical conditions as the extant *Azolla*. This explains part of the 8‰ enrichment. Secondly, elevated CO_2 levels substantially enhance *Azolla* growth rates, as has been shown in the cultivation experiments (see section 4.1.1). Increased growth rates decreases isotopic fractionation (Hayes *et al.*, 1999), possibly explaining the higher $\delta^{13}C$ values for the ω20 diols in the ACEX

sediments, and counteracting the effect of higher CO_2 levels. Based on *Azolla* microspore massulae abundances in the core (~50 000 g^{-1} dry sediment), or 5.2 10^6 spores m^{-1} $year^{-1}$, high Eocene Arctic production rates are inferred. For comparison, it was estimated that a thick mat of 8 kg m^{-2} fresh biomass is needed to produce 380 000 microsporocarps and 85 000 megasporocarps per m^{-2} (Janes, 1998). The high ^{13}C values found here are also consistent with the high ^{13}C encountered in fish apatite by Waddell & Moore (2008). These were found to reflect extremely high primary production, which resulted in enhanced growth rates and decreased isotopic fractionation, followed by burial of fish bones with ^{13}C enriched organic matter.

4.3 Impact of the Arctic *Azolla* bloom on CO_2 drawdown

Using sedimentary TOC content and sedimentation rates the potential CO_2 drawdown during the *Azolla* interval can be estimated. Combining TOC values of 4 wt% (Fig. 6) with a mass accumulation rate of 35 g m^{-2} $year^{-1}$ results in a net carbon burial rate of 1.4 gC m^{-2} $year^{-1}$. Recently, Knies *et al.* (2008) estimated a maximum primary palaeoproductivity during the *Azolla* phase of 120 gC m^{-2} $year^{-1}$, using sedimentary organic carbon content, correcting for decomposition in the water column, burial efficiency, and dilution by inorganic sediment (Knies & Mann, 2002). Our experiments show average production rates for extant *Azolla* under ambient conditions: 4.5–5 g dry weight per m^2 day^{-1} or 2 gC m^{-2} day^{-1}. A production rate of 2 gC m^{-2} day^{-1} would have yielded 120 gC m^{-2} within 2 months, a primary production estimate of 120 gC m^{-2} $year^{-1}$ thus seems reasonable, albeit a bit on the low side given Eocene pCO_2 levels and associated enhanced *Azolla* growth. Also the prolonged photoperiod during the Arctic summer would have stimulated higher *Azolla* production. Estimated primary productivity of 120 gC m^{-2} $year^{-1}$ in combination with a net carbon burial rate of 1.4 gC m^{-2} $year^{-1}$, demonstrates a fairly low burial efficiency of 1.2%. Hence, despite the water column anoxia extensive biodegradation must have occurred either during transport in the water column or at the sediment–water interface, or over time within the sediments.

The preservation of diols is better than that of for instance fatty acids, neutral lipids, sterols, *n*-alkanols, and *n*-alkanes (Sun & Wakeham, 1994), but these compounds are probably more susceptible to degradation than spores. If the preservation of diols reflects the average degree of preservation of *Azolla*-derived organic matter, comparison of the Eocene Arctic diol fluxes with current *Azolla* diol production rates will give a minimum estimate of *Azolla* growth. Diol (ω20 C_{30}–C_{36}) concentrations in the ACEX core sum up to 4.5 μg g^{-1} sediment, or 80 μg g^{-1} TOC. In cultured extant *Azolla* the total diol concentration for fresh *Azolla* amounts to 480 μg g^{-1} (dry weight) *Azolla* or 190 μg gC^{-1} in *Azolla*. If all organic constituents in *Azolla* would preserve equally well, this would indicate that about 40% of the Eocene TOC would be derived from *Azolla*. Based on the palynological composition (Brinkhuis *et al.*, 2006), this is an underestimate.

CO_2 fixation by *Azolla* and subsequent burial of *Azolla*-derived organic matter has direct consequences for the carbon inventory of the atmosphere–ocean system. The burial of *Azolla*-derived organic matter is assumed to occur in conjunction with ongoing cycling of carbon. To quantify the effect of enhanced organic carbon storage in the Eocene Arctic Basin on atmospheric pCO_2 levels and ocean-atmosphere partitioning, equation 1 should be solved.

$$\Delta pCO_2 = \int_{\Sigma C_1}^{\Sigma C_2} \frac{pCO_2}{\left(I_A + \frac{I_O}{R_{global}}\right)} d\Sigma C \qquad (1)$$

where ΔpCO_2 is the change in atmospheric partial CO_2 pressure resulting from a perturbation in the global carbon inventory. $\Delta\Sigma C$ represents the total carbon perturbation: the amount of carbon added to or removed from the inventory. I_A is the carbon inventory of the atmosphere, I_O is the carbon inventory of the ocean and R_{global} is the average Revelle buffer factor (Revelle & Suess, 1957). Goodwin *et al.* (2007) showed that this equation can be solved analytically. Here we apply and compare two analytical methods to solve equation 1. The first analytical method used follows a linear approximation (e.g. Archer, 2005) described by equation 2:

$$\Delta pCO_2 = \frac{1}{M}\left(1 + \frac{I_O}{R_{global} I_A}\right)^{-1} \Delta\Sigma C \qquad (2)$$

where M represents the molar volume of the atmosphere. I_A, I_O and R_{global} are evaluated at a steady-state carbon partitioning between ocean and atmosphere, assuming a mean annual global SST of 20 °C, with total air–sea carbon levels corresponding to Eocene values (Table 2). This relation is found to be valid if either the change in carbon inventory is small or as long as the value of R_{global} increases when charge neutral carbon is extracted from the system.

Table 2 Calculated values for I_A, I_O, R_{global}, and I_B, for two sets of Eocene conditions

	I_A (gC)	I_O (gC)	I_B (gC)*	R_{global}
Eocene ~800 ppm†	1.70 10^{18}	1.491 10^{20}	1.26 10^{19}	13.7
Eocene ~2000 ppm‡	4.25 10^{18}	1.901 10^{20}	1.49 10^{19}	17.8

*I_B is calculated as $I_B = I_O/R_{global} + I_{aA}$, using a mean annual SST of 20 °C and salinity of 35 psu.

†800 ppm: sea surface alkalinity of 2800 μmol eq kg^{-1}, after Pearson & Palmer (2000).

‡2000 ppm: sea surface alkalinity of 3400 μmol eq kg^{-1}, after Pearson & Palmer (2000).

The second analytical solution has been found to better approximate carbon emissions up until 5000 GtC (corresponding to a pCO_2 level of 1050 ppm, starting from 280 ppm) (Goodwin *et al.*, 2007). This solution makes use of a total air–sea 'buffered' carbon inventory, I_B (Goodwin *et al.*, 2007). The buffered amount of carbon represents the CO_2 available for redistribution between the atmosphere and the ocean. I_B is assumed to be constant. This last approximation can also be used for larger emissions as it allows for variation in R_{global}.

$$pCO_2 = P_i e^{\frac{\Delta\Sigma C}{I_B}} \quad (3)$$

P_i is the initial partial pressure of carbon dioxide. Each of the analytical methods is applied to two different sets of Eocene initial pCO_2 conditions. Despite the extensive biodegradation, after a period of 160 000 years still 224 kg m^{-2} organic carbon, based on net carbon flux of 1.4 gC m^{-2} $year^{-1}$, accumulated. For the entire Eocene Arctic basin (4.0 10^6 km^2), provided TOC contents are laterally uniform at 4%, this would amount to 9.0 10^{17} gC or 3.3 10^{18} gCO_2. Alternatively the *Azolla* phase also included the unrecovered sections below 11X until 15X, which using an average accumulation rate of 1.27 cm kyr^{-1} corresponds to a duration of 1.2 Ma. This maximum extent of the sedimentary sequence corresponds to a carbon storage of 3.5 10^{18} gC or 13 10^{18} gCO_2.

Based on Eocene partial CO_2 pressure, and corresponding Eocene alkalinity (Pearson & Palmer, 2000), the atmospheric I_A, oceanic I_O, and the Revelle buffer factor can be calculated. The total amount of buffered carbon (I_B) is then computed for the Eocene case (Table 2). The first Eocene case uses an initial partial CO_2 pressure of 800 ppm, with an alkalinity of 2800 μmol kg^{-1} (Pearson & Palmer, 2000 estimate for ~49 Ma). The second case assumes a 2000-ppm pCO_2 and corresponding alkalinity of 3400 μmol kg^{-1} (Pearson and Palmer estimate for ~53 Ma) (Table 2). Both are evaluated for two estimates of organic carbon accumulation in the *Azolla* interval (Table 2). In Fig. 8 the two analytical solutions are shown for the two different Eocene scenarios. Differences in I_B lead to differences in decrease in atmospheric pCO_2, following equation 3, which explains why the impact of sequestration of similar amounts of carbon burial results in different effects on pCO_2 levels. For both scenarios, R_{global} initially decreases as charge neutral CO_2 is extracted from the air–sea system, making the linear approximation less suitable for the larger perturbations in ΔΣC. Still, the two different analytical approaches (linear and exponential) give very similar results (Table 3; Fig. 8) for the same Eocene scenarios. In absolute amounts, CO_2 drawdown is higher in the 2000 ppm case than in the 800 ppm. Relatively, however, drawdown falls in the same range: ~7% for 9.0 10^{17} gC and ~25% for storage of 3.5 10^{18} gC. The close match between the two is explained by the fact that for both the 800 and the 2000 ppm cases a similar ocean carbon inventory (I_O/R_{global}) of ~1.1 10^{19} gC was inferred. Based on our calculations sequestration of 9.0 10^{17} gC in the Arctic Basin had the potential to lower the concentration of atmospheric pCO_2 by *c.* 55–120 ppm When an estimated total extent of the *Azolla* interval of ~15 m is used, an even higher CO_2 drawdown of 195–470 ppm is calculated, based on 3.5 10^{18} gC storage. However, the exact magnitude of atmospheric CO_2 drawdown was also influenced by carbon cycle related feedback mechanisms. For instance, storage of carbon

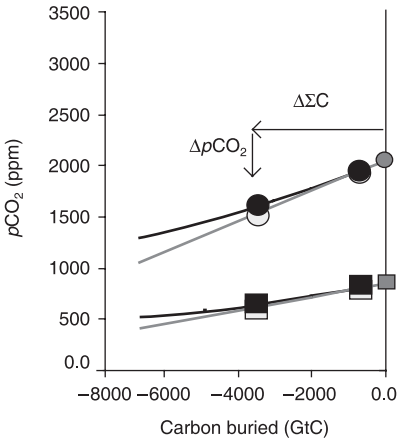

Fig. 8 Atmospheric pCO_2 against emission/drawdown of –6500 GtC. Light grey lines: pCO_2 responds linearly with emissions, as described by equation 2. Dark grey lines: pCO_2 decreases exponentially with carbon drawdown, following equation 3. Calculated pCO_2 levels for the different carbon storages (0.9 10^{18} and 3.5 10^{18} gC, respectively) are plotted in white for the linear and in black for the exponential solution. For both analytical solutions I_A, I_O, R_{global}, and I_B are evaluated at a steady state at the two chosen Eocene pCO_2 levels of 800 and 2000 ppm Sea surface salinity is set to 35 psu, global SST to 20 °C, Eocene pCO_2 and alkalinity are obtained from Pearson & Palmer (2000).

Table 3 Response of atmospheric pCO_2 to calculated burial of organic matter during the *Azolla* interval for two different Eocene initial partial pressures estimates

	1. Linear	1. Linear	2. Exponential	2. Exponential
	pCO_2 drawdown (burial of 0.9 10^{18} gC)	pCO_2 drawdown (burial of 3.5 10^{18} gC)	pCO_2 drawdown (burial of 0.9 10^{18} gC)	pCO_2 drawdown (burial of 3.5 10^{18} gC)
Eocene ~800 ppm	57 ppm	220 ppm	55 ppm	195 ppm
Eocene ~2000 ppm	120 ppm	470 ppm	120 ppm	420 ppm

results in an increase in ocean water pH and an increase in CO_3^{2-} concentration. This perturbs the $CaCO_3$ cycle by increasing global burial rates of $CaCO_3$. Such a perturbation in turn acts to buffer changes in oceanic pH and thus reduces amplitude of atmospheric pCO_2 changes. On the other hand, a temperature feedback (i.e. cooling) would increase solubility of CO_2 in the ocean and thus further decrease atmospheric pCO_2 levels. On longer timescales (~100 kyr), reduced silicate weathering would possibly counteract CO_2 storage to some extent.

Forty per cent of the calculated 55–470 ppm CO_2 drawdown is directly attributable to *Azolla* production, because 40% of TOC consists of *Azolla*-derived carbon. Indirectly, however, nitrogen fixation by organisms associated with *Azolla* could have increased the regional fixed nitrogen availability. The excess fixed nitrogen would have been available for other organisms in the Arctic Basin as well. If transported from the basin this excess fixed nitrogen could have increased productivity in an even larger area. In this way, Arctic *Azolla* blooms could also have enhanced carbon drawdown indirectly in a much larger area potentially contributing even more to decreasing CO_2 levels in the Eocene.

5. SUMMARY

Palaeoenvironmental reconstructions of the Middle Eocene Arctic Ocean suggest a warm, humid environment, with aquatic floating *Azolla* inhabiting a freshwater layer capping more saline Arctic bottom waters. The high resolution record of *Azolla* massulae counts as obtained from sediments recovered during IODP expedition 302 at the Lomonosov Ridge confirm the cyclic pattern of Eocene *Azolla* abundances. Based on bulk sediment analyses, including high organic carbon contents, low C/S ratios, overall, euxinic bottom-water conditions are inferred, which is consistent with previous reports (Knies *et al.*, 2008). Bulk $\delta^{15}N$ values are persistently low (<–1‰) and mark the importance of nitrogen fixation as a source of fixed N in the stratified basin. The high C_{org}/N_{org} ratios point toward extensive selective degradation of nitrogen-rich organic compounds, despite the continuous anoxic bottom waters. Given the low reconstructed burial efficiency of 1.2%, considerable biodegradation must indeed have occurred despite the reconstructed euxinic bottom-water conditions. Stable isotope analyses ($\delta^{13}C$) of extracted biomarkers for *Azolla* revealed that values in the Eocene differ from the present day by 3‰ (β-sitosterol) and 8‰ (1,ω-20 C_{30}–C_{36} diols), respectively. These differences are partly due to the different composition of the Eocene global DIC reservoir but also suggest that *Azolla* primary production rates were much higher in the Eocene than nowadays, leading to less ^{13}C fractionation.

The first results of culturing experiments of extant *Azolla* mimicking Eocene pCO_2 conditions show doubling growth rates of *Azolla filiculoides* in the 1910 ppm atmospheric pCO_2 treatment compared to the control of 340 ppm. Under Eocene pCO_2 conditions, *Azolla* could thus reproduce at higher rates than under present-day CO_2 concentrations and could fix carbon at higher rates.

A minimum and maximum estimate of carbon storage in the Arctic for the *Azolla* interval has been obtained. Calculations are based on extrapolation of the organic carbon accumulation rates over the entire Eocene Arctic basin, leaving out the Nordic Sea areas. The maximum organic carbon storage of 3.5 10^{18} gC is calculated based on accumulation rates of 12.7 cm kyr^{-1} and a time interval of 1.2 Ma for the *Azolla* interval. The minimum estimate is based on only the recovered ACEX sediments as age control and an associated accumulation rate of 2.43 cm kyr^{-1}, in which case still a substantial amount of 9.0 10^{17} gC stored is computed. Storage of 3.5 10^{18} g carbon roughly corresponds to a 195–470 ppm and 9.0 10^{17} gC to a 55–120 ppm CO_2 drawdown. It has been estimated that the growth of *Azolla* itself contributed at least 40% to this carbon drawdown via net carbon fixation and subsequent sequestration.

ACKNOWLEDGEMENTS

This research used samples and data provided by the Integrated Ocean Drilling Program (IODP). Funding for this research was provided by the DARWIN centre for Biogeology. Authors would like to thank StatoilHydro for general support and additional samples from exploration wells. We would also like to thank Gijs Nobbe and Rinske Knoop for technical laboratory assistance.

REFERENCES

Allen SG, Idso SB, Kimball BA, Anderson MG (1988) Interactive effects of CO_2 and environment on photosynthesis of Azolla. *Agricultural and Forest Meteorology* **42**, 209–217.

Altabet MA, Francois R (1994) Sedimentary nitrogen isotopic ratio as a recorder for surface ocean nitrate utilization. *Global Biogeochemical Cycles* **8**, 103–116.

Archer D (2005) The fate of fossil fuel in geologic time. *Journal of Geophysical Research* **110**, C09S05.

Backman J, Moran K, McInroy DB, Mayer LA, Expedition-Scientists Arctic Coring Expedition (ACEX) (2006) *Proceedings of the Integrated Ocean Drilling Program* **302**. (doi:10.2204/iodp.proc.302.2006, IODP Management International, College Station Texas).

Backman J, Jakobsson M, Frank M, Sangiorgi F, Brinkhuis H, Stickley C, O'Regan M, Løvlie R, Pälike H, Spofforth D, Gattacecca J, Moran K, King J, Heil C (2008) Age model and core-seismic integration for the Cenozoic Arctic Coring Expedition sediments from the Lomonosov Ridge. *Paleoceanography* **23**, PA1S03.

Berner RA (1984) Sedimentary pyrite formation: an update. *Geochimica and Cosmochimica Acta* **48**, 605–615.

Braun-Howland EB, Nierzwicki-Bauer SA (1990) Azolla–Anabaena azollae symbiosis: biochemistry, ultrastructure and molecular biology. In: *Handbook of Symbiotic Cyanobacteria* (ed. Rai AN), pp. 65–118. Boca Raton, FL.

Brinkhuis H, Schouten S, Collinson ME, Sluijs A, Sinninghe Damsté JS, Dickens GR, Huber M, Cronin TM, Onodera J, Takahashi K, Bujak JP, Stein R, van der Burgh J, Eldrett JS, Harding IC, Lotter AF, Sangiorgi F, van Konijnenburg-van Cittert H, de Leeuw JW,

Matthiessen J, Backman J, Moran K and the Expedition 302 Scientists (2006) Episodic fresh surface waters in the Eocene Arctic Ocean. *Nature* **441**, 606–609.

Bunn SE, Boon PI (1993) What sources of organic carbon drive food weds in Billabongs: a study based on stable isotope analysis. *Oecologia* **96**, 85–94.

Cary PR, Weerts PGJ (1992) Growth and nutrient composition *of Azolla pinnata* R. Brown and *Azolla filiculoides* Lamarck as affected by water temperature, nitrogen and phosphorus supply, light intensity and pH. *Aquatic Botany* **43**, 163–180.

Cline JD, Kaplan IR (1975) Isotopic fractionation of dissolved nitrate during dentrification in the eastern tropical north pacific Ocean. *Marine Chemistry* **3**, 271–299.

Collinson ME (2002) The ecology of Cainozoic ferns. *Review of Palaeobotany and Palynology* **119**, 51–68.

Collinson ME, Barke J, van der Burg J, van Konijnenburg-van Cittert JHA (2008) *Review of Palaeobotany and Palynology*, accepted.

Eldrett JS, Harding IC, Firth JV, Roberts AP (2004) Magnetostratigraphic calibration of Eocene-Oligocene dinoflagellate cyst biostratigraphy from the Norwegian-Greenland Sea. *Marine Geology* **204**, 91–127.

Estes R, Hutchinson JH (1980) Eocene lower vertebrates from Ellesmere Island, Canadian Arctic Archipelago. *Palaeogeography, Palaeoclimatology, Palaeoecology* **30**, 325–347.

Gächter R, Meyer JS, Mares A (1988) Contribution of bacteria to release and fixation of phosphorus in lake sediments. *Limnology and Oceanography* **33**, 1542–1558.

Glebovsky VY, Kaminsky VD, Minakov AN, Merkuriev SA, Childers VA, Brozena JM (2006) Formation of the Eurasia Basin in the Arctic Ocean as inferred from geohistorical analysis of the anomalous magnetic field. *Geotectonics* **40**, 263–281.

Goodwin P, Williams RG, Follows MJ, Dutkiewicz S (2007) Ocean-atmosphere partitioning of anthropogenic carbon dioxide on centennial timescales. *Global Biogeochemical Cycles* **21**, GB1012.

Gradstein FM, Luterbacher HP, Ali JR, Brinkhuis H, Gradstein FM, Hooker JJ, Monechi S, Ogg JG, Powell J, Röhl U, Sanfilippo A, Schmitz B. (2004) The paleogene period. In: *A Geologic Time Scale* (eds Gradstein FM, Ogg JG, Smith AG). pp. 396. Cambridge University Press, Cambridge, UK.

Greenwood DR, Wing SL (1995) Eocene continental climates and latitudinal temperature gradients. *Geology* **23**, 1044–1048.

Hayes JM (2001) Fractionation of carbon and hydrogen isotopes in biosynthetic processes. *Stable Isotope Geochemistry* **43**, 225–277.

Hayes JM, Strauss H, Kaufman AJ (1999) The abundance of ^{13}C in marine organic matter and isotopic fractionation in the global biogeochemical cycle of carbon during the past 800 Ma. *Chemical Geology* **161**, 103–125.

Huber M, Sloan LC, Shellito CJ (2003) Early Paleogene oceans and climate: a fully coupled modeling approach using the NCAR CCSM. In *Causes and Consequences of Globally Warm Climates in the Early Palaeogene* (eds Wing SL *et al.*). Special Papers Geological Society of America, **369**, 25–47.

Idso SB, Allen SG, Anderson MG, Kimball BA (1989) Atmospheric CO_2 enrichment enhances survival of *Azolla* at high temperatures. *Environmental and Experimental Botany* **29**, 337–341.

Jahren AH, Sternberg LSL (2003) Humidity estimate for the middle Eocene Arctic rain forest. *Geology* **31**, 463–466.

Jakobsson M, Backman J, Rudels B, Nycander J, Frank M, Mayer M, Jokat W, Sangiorgi F, O'Regan M, Brinkhuis H, King J, Moran K (2007) The early Miocene onset of a ventilated circulation regime in the Arctic Ocean. *Nature* **447**, 986–990.

Janes R (1998) Growth and survival of *Azolla filiculoides* in Britain, II. Sexual reproduction. *New Phytologist* **138**, 377–384.

Kingston HM, Haswell SJ (1997) *Microwave Enhanced Chemistry*: *Fundamentals, Sample Preparation and Applications*. American Chemical Society, Washington DC.

Knies J, Mann U (2002) Depositional environment and source rock potential of Miocene strata from the central Fram Strait: introduction of a new computing tool for simulating organic facies variations. *Marine Petroleum Geology* **19**, 811–828.

Knies J, Mann U, Popp BN, Stein R, Brumsack HJ (2008) Surface water productivity and paleoceanographic implications in the Cenozoic Arctic Ocean. *Paleoceanography* **23**, PA1S16.

Koizumi H, Kibe T, Mariko S, Ohtsuka T, Nakadai T, Mo W, Toda H, Seiichi N, Kobayashi K (2001) Effects of free-air CO_2 enrichment (FACE) on CO_2 exchange at the flood-water surface in a rice paddy field. *New Phytologist* **150**, 231–239.

Kurtz AC, Kump LR, Arthur MA, Zachos JC, Paytan A (2003) Early Cenozoic decoupling of the global carbon and sulfur cycles. *Paleoceanography* **18**(4), 1090, doi: 10.1029/2003PA000908.

Kuypers MMM, Sliekers AO, Lavik G, Schmid M, Jorgensen BB, Kuenen JG, Sinninghe Damsté JS, Strous M, Jetten MSM (2003) Anaerobic ammonium oxidation by annamox bacteria in the Black Sea. *Nature* **422**, 608–611.

Kuypers MMM, van Breugel Y, Schouten S, Erba E, Sinninghe Damsté JS (2004). N_2-fixing cyanobacteria supplied nutrient N for Cretaceous oceanic anoxic events. *Geology* **32**, 853–856.

Manabe S (1997) Early development in the study of greenhouse warming: the emergence of climate models. *Ambio* **26**, 47–51.

Manum SB, Boulter MC, Gunnarsdottir H, Rangnes K, Scholze A (1989) Eocene to Miocene palynology of the Norwegian Sea (ODP Leg 104). In *Proceedings of Ocean Drilling Program, Scientific Results 104* (eds Eldholm O Thiede J Taylor E *et al.*) College Station, TX. 611–662.

Marschner H (1995) *Mineral Nutrition of Higher Plants*, 2nd edn. Academic Press, London.

Minagawa M, Wada E (1986) Nitrogen isotope ratios of red tide organisms in the East China Sea: a characterization of biological nitrogen fixation. *Marine Chemistry* **19**, 245–259.

Montoya JP, Holl CM, Zehr JP, Hansen A, Villareal TA, Capone DG (2004) High rates of N_2 fixation by unicellular diazotrophs in the oligotrophic Pacific Ocean. *Nature* **430**, 1027–1031.

Moran K, Backman J, Brinkhuis H, Clemens SC, Cronin T, Dickens GR, Eynaud F, Gattacceca J, Jakobsson M, Jordan RW, Kaminski M, King J, Koc N, Krylov A, Martinez N, Matthiessen J, McInroy D, Moore TC, Onodera J, O'Regan M, Pälike H, Rea B, Rio D, Sakamoto T, Smith DC, Stein R, St John K, Suto I, Suzuki N, Takahashi K, Watanabe M, Yamamoto M, Farrell J, Frank M, Kubik P, Jokat W, Kristoffersen Y (2006) The Cenozoic palaeoenvironment of the Arctic Ocean. *Nature* **441**, 601–605.

Moretti A, Siniscalco Gigliano G (1988) Influence of light and pH on growth and nitrogenase activity on temperate-grown *Azolla*. *Biology and Fertility of Soils* **6**, 131–136.

Pagani M, Zachos JC, Freeman KH, Tipple B, Bohaty S (2005) Marked decline in atmospheric carbon dioxide concentrations during the Paleogene. *Science* **309**, 600–603.

Pearson PN, Palmer MR (2000) Atmospheric carbon dioxide concentrations over the past 60 million years. *Nature* **406**, 695–699.

Pearson PN, Ditchfield PW, Singano J, Harcourt-Brown KG, Nicholas CJ, Olsson RK, Shackleton NJ, Hall MA (2001) Warm tropical sea surface temperatures in the Late Cretaceous and Eocene epochs. *Nature* **413**, 481–487.

Peters GA, Meeks JC (1989) The *Azolla–Anabaena* symbiosis: basic biology. *Annual Reviews in Plant Physiology and Plant Molecular Biology* **40**, 193–210.

Powers LA, Werne JP, Johnson TC, Hopmans EC, Sinninghe Damsté JS, Schouten S (2004) Crenarchaeotal membrane lipids in lake

sediments: a new Paleotemperature proxy for continental paleoclimate reconstruction? *Geology* **32**, 613–616.
Rai V, Tiwari SP, Rai AK (2001) Effects of NaCl on nitrogen fixation of unadapted and NaCl adapted *Azolla pinnata–Anabaena azollae*. *Aquatic Botany* **71**, 109–117.
Reuveni J, Gale J, Zeroni M (1997) Differentiating day from night effects of high ambient CO_2 on the gas exchange and growth of *Xanthium strumarium* L. exposed to salinity stress. *Annual Botany* **9**, 191–196.
Revelle R, Suess HE (1957) Carbon dioxide exchange between atmosphere and ocean and the question of an increase of atmospheric CO_2 during the past decades. *Tellus* **9**, 18–27.
Royer DL, Wing SL, Beerling DJ, Jolley DW, Koch PL, Hickey LJ, Berner RA (2001) Paleobotanical evidence for near present day levels of atmospheric CO_2 during part of the Tertiary. *Science* **292**, 2310–2313.
Sah RN, Goyal SS, Rains DW (1989) Interactive effects of exogenous combined nitrogen and phosphorus on growth and nitrogen fixation by *Azolla*. *Plant and Soil* **117**, 1–8.
Sangiorgi F, van Soelen EE, Spofforth DJA, Pälike H, Stickley CE, St John K, Koç N, Schouten S, Sinninghe Damsté JS, Brinkhuis H (2008) Cyclicity in the middle Eocene central Arctic Ocean sediment record: orbital forcing and environmental response. *Paleoceanography* **23**, PA1S08.
Saunders RMK, Fowler K (1993) The supraspecific taxonomy and evolution of the fern genus *Azolla* (Azollaceae). *Plant Systematics and Evolution* **184**, 175–193.
Schouten S, Klein Breteler WCM, Blokker P, Schoot N, Rijpstra WIC, Grice K, Baas M, Sinninghe Damsté JS (1998) Biosynthetic effects on the stable carbon isotopic compositions of algal lipids: implications for deciphering the carbon isotopic biomarker record. *Geochimica et Cosmochimica Acta* **62**, 1397–1406.
Schouten S, Hopmans EC, Schefuß E, Sinninghe Damsté JS (2002) Distributional variations in marine crenarchaeotal membrane lipids: a new tool for reconstructing ancient sea water temperatures? *Earth and Planetary Science Letters* **204**, 265–274.
Schubert CJ, Calvert SE, Stein R (2001) Tracking nutrient and productivity variations over the last deglaciation in the Arctic Ocean. *Paleoceanography* **16**, 199–211.
Scotese CR, Gahagan LM, Larson RL (1988) Plate tectonic reconstructions of the Cetaceous and Cenozoic ocean basins. *Tectonophysics* **155**, 27–48.
Skipski VP, Smolowe AF, Sullivan RC, Barclay M (1965) Separation of lipid classes by thin-layer chromatography. *Biochimica et Biophysica Acta* **196**, 386–396.
Sluijs A, Schouten S, Pagani M, Woltering M, Brinkhuis H, Sinninghe Damsté JS, Dickens GR, Huber M, Reichart GJ, Stein R, Matthiessen J, Lourens LJ, Pedentchouk N, Backman J, Moran K & the Expedition 302 Scientists (2006) Subtropical Arctic Ocean temperatures during the Palaeocene/Eocene thermal maximum. *Nature* **441**, 610–613.
Speelman EN, Reichart GJ, de Leew JM, Rijpstra WIC, Sinninghe Damsté JS (2009) Biomarker lipids of the freshwater fern *Azolla* and its fossil counterpart from the Eocene Arctic Ocean. *Organic Geochemistry* in press.
Stein R, Boucsein B, Meyer H (2006) Anoxia and high primary production in the Paleogene central Arctic Ocean: first detailed records from Lomonosov Ridge. *Geophysics Research. Letters* **33**, LI8606.
Stickley CE, Koc N, Brumsack HJ, Jordan RW, Suto I (2008) A siliceous microfossil view of middle Eocene Arctic paleoenvironments: a window of biosilica production and preservation. *Paleoceanography* **23**, PA1S14.
Sun M-Y, Wakeham SG (1994) Molecular evidence for degradation and preservation of organic matter in the anoxic Black Sea Basin. *Geochimica et Cosmochimica Acta* **58**, 3395–3406.
Tripati A, Backman J, Elderfield H, Ferretti P (2005) Eocene bipolar glaciation associated with global carbon cycle changes. *Nature* **436**, 341–346.
Van Cappellen P, Ingall ED (1994) Benthic phosphorus regeneration, net primary production, and ocean anoxia: a model of the coupled marine biogeochemical cycles of carbon and phosphorus. *Paleoceanography* **9**, 677–692.
Waddell LM, Moore TC (2008) Salinity of the Eocene Arctic Ocean from oxygen isotope analysis of fish bone carbonate. *Paleoceanography* **23**, PA1S12.
Wagner GM (1997) Azolla: a review of its biology and utilization. *The Botanical Review* **63**, 1–26.
Yapp CJ (2004) Fe (CO_3) OH in goethite from a mid-latitude North American oxisol: estimate of atmospheric CO_2 concentration in the early Eocene 'climatic optimum.' *Geochimica et Cosmochimica Acta* **68**, 935–947.
Zachos JC, Pagani M, Sloan LC, Thomas E, Billups K (2001) Trends, rhythms, and aberrations in global climate 65 Ma to present. *Science* **292**, 686–693.
Zachos JC, Dickens GR, Zeebe RE (2008) An early Cenozoic perspective on greenhouse warming and carbon-cycle dynamics. *Nature* **451**, 279–283.
Zeebe RE, Wolf-Gladrow D, eds. (2001) CO_2 *in Seawater: Equilibrium, Kinetics, Isotopes*. Elsevier Oceanography Series. **65**.